Supplement–Upper Limits on the Stochastic Gravitational-Wave Background from Advanced LIGO's First Observing Run

In this supplement we describe in more detail how the data in the main text are analyzed. Data used in the analysis are from times when both detectors are in a low-noise observing mode. We exclude certain times and frequencies based on auxiliary channels that established them as instrumental effects within the detectors.

We remove times due to known instrumental artifacts, such as radio frequency (RF) glitching and electronics saturations [1], or due to simulated signals (referred to as hardware injections) generated by coherently moving the interferometer mirrors [2]. We also exclude segments associated with detections of gravitational waves. Data are also excluded when the detectors' noise power spectra vary by more than 20% over the course of three 192s segments. This cut is performed to remove non-stationary noise, and has been used in previous analyses [3]. A dedicated study has verified that removing variations of 20% provides a close-to-optimal balance between the false positive and false negative rates. The total live time with all vetoes applied, for 192s segments, is 29.85 days. These cuts remove 35% of the time-series data.

We exclude frequencies known to be associated with instrumental artifacts, such as vibrations of the test mass suspensions and calibration lines. We also remove frequencies that are known to be instrumentally correlated between the two LIGO detectors. As an example, we detected a comb-like structure (a series of lines evenly spaced in frequency) at half Hz frequencies with 1 Hz separation. This structure was coherent between the two sites and subsequently observed in auxiliary channels. The contributing frequency bins were not included in the analysis. The frequency domain cuts remove 21% of the observing band within each segment.

To verify the data analysis cuts described above, we introduce an artificial time shift of 1 s between the two sites. This effectively blinds the analysis by removing correlations due to a broadband gravitational-wave signal, while maintaining instrumental correlations with coherence times greater than 1 s. This method also allows us to identify additional instrumental artifacts that are not identified using the cuts above, without biasing our analysis of the data. Upon studying the time-shifted data with the analysis cuts described above, we find no excess correlation, which is consistent with statistical expectations of uncorrelated Gaussian noise.

As a test of the detectors and the analysis pipeline, we simulate a strong stochastic signal both by a hardware injection and by a software injection (made by adding a coherent signal to the data streams). The injected background signals were isotropic and Gaussian, with an amplitude of $\Omega_0 = 8.7 \times 10^{-5}$ and a duration of 600 s. Both types of injections were successfully recovered within 1 σ uncertainty: the hardware injection measured $(8.8 \pm 0.6) \times 10^{-5}$ and the software injection measured $(9.0 \pm 0.6) \times 10^{-5}$.

Finally, we study the possibility of correlated noise between H1 and L1 so that we may be confident that the systematic error in our measurements is negligible. After accounting for narrowband correlation detector artifacts arising from digital systems, we estimate the contamination from the environment. Previous investigations have identified geophysical Schumann resonances as the most likely source of correlated environmental noise [4, 5]. Excitations in the spherical shell cavity formed between the surface of the Earth and the ionosphere cause magnetic fields to be correlated over great distances, comparable to the separation between H1 and L1. The magnetic fields, in turn, can couple mechanically to the test mass through the suspension system or electronically [5]. In order to ascertain the systematic error from environmental correlated noise, we construct a correlated noise budget. We employ a number of conservative assumptions in order to estimate the worst-case-scenario contamination.

The first step is to measure the frequency-dependent coupling of the detector to ambient magnetic fields using external coils as an actuator [4, 5]. It is not practical to induce fields that act on the entire detector simultaneously, so we measure the coupling at each test mass. Next, we use magnetometers to measure the magnetic coherence between the two sites. Using the method described in [4, 5], we combine the magnetic cross-power spectra and the coupling functions to estimate the worst-case correlated noise from Schumann res-

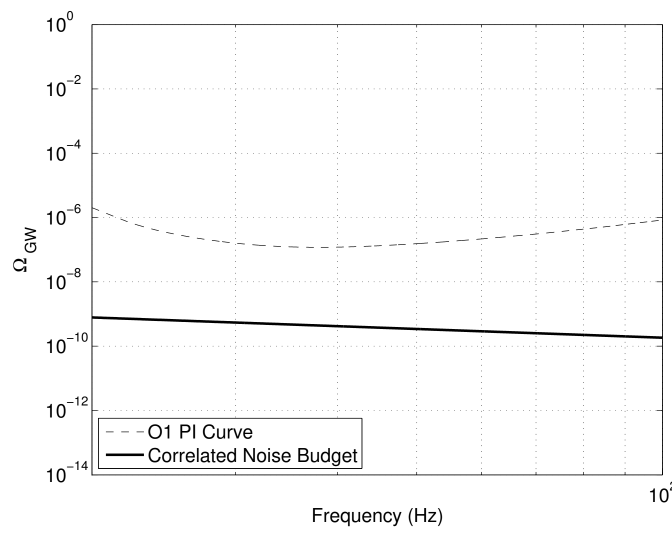

FIG. 1. We show the O1 power-law integrated curve (PI curve) along with the correlated noise budget as described in the text. The noise budget falling below the O1 PI curve indicates that correlated noise does not affect the O1 analysis.

onances $\Omega_{\rm noise}(f)$. Our conservative noise budget for O1 corresponds to the solid black curve in Figure 1. This curve is obtained by fitting a power law to the magnetic noise budget. We compare the noise budget to the power-law integrated energy density spectrum (dashed black curve) [6], which represent the statistical uncertainty of the stochastic search. During O1, the correlated noise is sufficiently low as to be ignored, contributing much less than one sigma. (If the correlated noise estimate was significant, the noise budget would be comparable to or in excess of the dashed curve in the region of ~20-30 Hz.) Work is ongoing to monitor and mitigate correlated noise for future.

[1] B. P. Abbot *et al.*, Class. Quantum Grav. **33**, 134001 (2016).

[2] C. Biwer *et al.*, `https://dcc.ligo.org/LIGO-P1600285/public`.

[3] J. Aasi *et al.*, Physical Review Letters **113**, 231101 (2014).

[4] E. Thrane, N. Christensen, and R. M. S. Schofield, Phys. Rev. D **87**, 123009 (2013).

[5] E. Thrane, N. Christensen, R. M. S. Schofield, and A. Effler, Phys. Rev. D **90**, 023013 (2014).

[6] E. Thrane and J. D. Romano, Phys. Rev. D **88**, 124032 (2013).